Molecular Therapy
Original Article

Targeting miR-21 with Sophocarpine Inhibits Tumor Progression and Reverses Epithelial-Mesenchymal Transition in Head and Neck Cancer

Wei Liu,[1,2,5] Beilei Zhang,[3,5] Guo Chen,[4,5] Wenjiao Wu,[1] Lin Zhou,[1] Yaru Shi,[1] Qi Zeng,[1] Yanqiu Li,[4] Youwei Sun,[4] Xingming Deng,[4] and Fu Wang[1]

[1]Engineering Research Center of Molecular and Neuro Imaging, Ministry of Education, School of Life Science and Technology, Xidian University, Xi'an, Shaanxi 710071, China; [2]Department of Hepatobiliary Surgery, Xijing Hospital, The Fourth Military Medical University, Xi'an, Shaanxi 710032, China; [3]Department of Gynecology and Obstetrics, Tangdu Hospital, The Fourth Military Medical University, Xi'an, Shaanxi 710038, China; [4]Department of Radiation Oncology, Emory University School of Medicine and Winship Cancer Institute, Emory University, Atlanta, GA 30322, USA

A major challenge for cancer chemotherapy is the development of safe and clinically effective chemotherapeutic agents. With its low toxicity profile, sophocarpine (SC), a naturally occurring tetracyclic quinolizidine alkaloid derived from *Sophora alopecuroides L*, has shown promising therapeutic properties, including anti-inflammatory, anti-nociceptive, and antivirus activities. However, the antitumor efficacy of SC and its underlying mechanisms have not been completely delineated. In the present study, the inhibitory effect of SC on head and neck squamous cell carcinoma (HNSCC) progression and possible mechanisms for this effect involving microRNA-21 (miR-21) regulation were investigated. By cell viability, Transwell, and wound healing assays, we show that SC effectively inhibited proliferation, invasion, and migration of HNSCC cells. Moreover, SC exerted its growth-inhibitory effect via the downregulation of miR-21 expression by blocking Dicer-mediated miR-21 maturation. Furthermore, SC treatment led to the increased expression of PTEN and p38MAPK phosphorylation as well as the reversal of epithelial-mesenchymal transition (EMT), which was rescued by ectopic expression of miR-21 in cells. Notably, SC dramatically repressed tumor growth without observable tissue cytotoxicity in a mouse xenograft model of HNSCC. Our findings offer a preclinical proof of concept for SC as a leading natural agent for HNSCC cancer therapy.

INTRODUCTION

Head and neck squamous cell carcinoma (HNSCC) is the sixth most fatal malignancy worldwide, with approximately 650,000 new cases and 350,000 HNSCC-related deaths occurring globally each year.[1] Although great medical advances for HNSCC treatment have been achieved in the past three decades, the overall survival rate of patients has not improved significantly due to second primary tumor recurrence.[2] Thus, understanding of the molecular events underlying HNSCC progression may disclose novel therapeutic targets in HNSCC.

In recent years, natural agents with potential anti-tumor properties have received greater attention in cancer prevention and treatment. A number of natural agents originating from various sources, such as microorganisms, fungi, and plants, have been used in the clinic or in clinical trials.[3] Classic examples of anti-cancer agents include citarabine, the first drug from a marine source, and paclitaxel, which is derived from a Chinese pacific yew plant. Other agents originating from microbial sources include doxorubicin, actinomycin D, bleomycin, and mitomycin C.[4] These drugs are characterized by a variety of mechanisms comprising interference with tumor angiogenesis, invasion, and metastasis, targeting cancer stem cells, modulating epigenetic modifications, and mediating microRNA expression.[5]

Sophocarpine (SC), a tetracyclic quinolizidine alkaloid, is one of the most abundant active ingredients in *Sophora alopecuroides L*. Previous studies have shown that SC possesses a number of pharmacological effects, including immuno-regulatory, anti-inflammatory, and anti-nociceptive activities.[6] Moreover, SC was found to alleviate hepatocyte steatosis by activating the AMPK signaling pathway and to preserve myocardial function from ischemia reperfusion via nuclear factor κB (NF-κB) inactivation.[7,8] However, the anti-tumor activities of SC on HNSCC and its underlying mechanisms are less understood.

MicroRNAs (miRNAs) are small noncoding RNAs that regulate gene expression through imperfect paring with their target mRNAs

Received 11 February 2017; accepted 12 May 2017;
http://dx.doi.org/10.1016/j.ymthe.2017.05.008.

[5]These authors contributed equally to this work.

Correspondence: Fu Wang, Engineering Research Center of Molecular and Neuro Imaging, Ministry of Education, School of Life Science and Technology, Xidian University, Xi'an, Shaanxi 710071, China.
E-mail: fwang@xidian.edu.cn
Correspondence: Xingming Deng, Department of Radiation Oncology, Emory University School of Medicine, Atlanta, GA 30322, USA; Winship Cancer Institute, Emory University, Atlanta, GA 30322, USA.
E-mail: xdeng4@emory.edu

and thereby result in mRNA cleavage or translation inhibition. The approximately 22-nt mature miRNAs were generated from the transcription of primary miRNA (pri-miRNA) and then processing of precursor miRNA (pre-miRNA) by the cleavage of the Drosha and Dicer enzyme.[9] miRNAs play crucial roles in a variety of biological processes, from cell proliferation, differentiation, and apoptosis to metabolism and senescence.[10] In addition, the abnormal expression profile of miRNAs is associated with different kinds of human cancers, indicating that miRNAs may function as oncogenes or tumor suppressors.[11] miR-21 is one of the most significantly overexpressed miRNAs in many different types of human cancers, including breast cancers, gastric cancers, colon cancers, and head and neck cancers.[12] It has been reported that miR-21 can promote the proliferation, invasion, and metastasis of cancer cells by targeting several tumor suppressor genes, including PTEN and PDCD4.[13,14] Therefore, targeting miR-21 and modulating its activity may open a promising route for cancer therapy.

In the present study, we demonstrated that SC was capable of inhibiting the proliferation, migration, and invasion of HNSCC cells through the blockage of Dicer-catalyzed miR-21 maturation and the involvement of the p38MAPK signaling pathway. Furthermore, SC efficiently led to the reversal of epithelial mesenchymal transition (EMT) in cancer cells and suppressed the growth of HNSCC cancer in vivo. Our results indicate that SC could be a potential lead compound for HNSCC treatment by targeting miR-21 expression.

RESULTS

SC Inhibits HNSCC Cell Proliferation, Invasion, and Migration

The anti-tumor activities of SC were determined in UM-SCC-22B and UM-SCC-47 cell lines. First, the cells were treated with different concentrations of SC (Figure 1A) for 48 hr, followed by analysis of cell viability using the CCK-8 assay. As shown in Figure 1B, SC showed a dose-dependent inhibition of cell proliferation. The half maximal concentration (IC_{50}) of SC in UM-SCC-22B or UM-SCC-47 cells is 1.067 μM or 1.536 μM, respectively.

Subsequently, we detected the impact of SC on the invasion of UM-SCC-22B and UM-SCC-47 cells by Transwell assays. The crystal violet-stained cells on the bottom surface of Transwell were washed and quantified at an optical density (OD) of 595 nm. The invasion rates of SC-treated cells were lower than the rates of DMSO-treated cells in a dose-dependent manner (Figure 1C). The same repression tendency of cell migration can also be observed in the wound scratch assay after increased concentrations of SC treatment (Figure 1D). Taken together, these results suggested that SC exhibited promising inhibitory activities on tumor cell proliferation, migration, and invasion.

SC Downregulates miR-21 Expression in HNSCC Cells

Accumulating evidence suggests that natural agents exert their anti-tumor activities via many different mechanisms, one of which is through modulating miRNAs expressions. So we tried to figure out whether miRNAs could be involved in the response of tumor cells treated by SC. Several known oncogenic or tumor-suppressive miRNAs,[15] including miR-15a, miR-34a, miR-10a, let-7a, miR-21, miR-99a, miR-9, miR-124a, and miR-155, were chosen to test. Real-time PCR was performed to examine the miRNA expression profiles in both SC-treated and untreated HNSCC cells (Figures 2A and 2B). Interestingly, compared with untreated cells, some of the tested miRNAs were downregulated, whereas some miRNAs were virtually unchanged in SC-treated cells. Of note, among the nine miRNAs screened, miR-21 exhibited a most strongly decreased response to SC treatment in both of the cell lines. To exclude the possibility of nonspecific modulation on miR-21 by SC, we treated the cells with another ten natural agents and found that these drugs had no obvious effect on miR-21 expression using a real-time PCR assay (Figure S1A). These results indicated that SC preferentially decreased miR-21 expression in HNSCC cells.

To further determine the effect of SC on miR-21 expression level, UM-SCC-22B and UM-SCC-47 cells were stimulated with different concentrations of SC (1 μM, 2 μM, and 4 μM) for 24 hr, and then real-time PCR was performed. As shown in Figure 2C, treatment with SC decreased miR-21 expression level in a dose-dependent manner, suggesting that SC could indeed downregulate miR-21 expression in HNSCC cells. What is more, combination treatment with miR-21 mimics and SC rescued the inhibitory effect on tumor cell viability (Figure 2D), invasion (Figure 2E), and migration (Figure 2F) induced by 4 μM SC alone. Taken together, these data indicate SC could inhibit HNSCC cell proliferation, invasion, and migration via downregulating miR-21 expression.

SC Represses miR-21 by Blocking Dicer Processing

On the basis of the inhibitory effect of SC on miR-21 expression, we would like to evaluate whether pre-miR-21 or pri-miR-21 expression was changed. As shown in Figure 3A, the expression level of pre-miR-21 increased in a dose-dependent manner after SC treatment in both of the cell lines, suggesting that SC might repress miR-21 by hindering the cleavage of pre-miR-21 to mature miRNA by Dicer. To further validate the hypothesis, we monitor the perturbation of Dicer processing pre-miR-21 to mature miR-21 in an in vitro Dicer-blocking assay. The pre-miR-21 was incubated with Dicer in the presence of increased concentrations of SC or absence of SC. As shown in Figure 3B, SC led to a dose-dependent reduction in miR-21 maturation, indicating that SC might bind to pre-miR-21 and thereby prevent Dicer processing. Moreover, SC treatment resulted in a dose-dependent reduction of pri-miR-21 expression, suggesting that SC upregulates pre-miR-21 by repressing pri-miR-21 expression (Figure S1B).

To verify the potential binding site of pre-miR-21 on Dicer that SC acts on, a wild-type and two-point-mutated pre-miR-21 oligos (Mut1 and Mut2) were synthesized (Figure 3C) and then transfected into the cell lines for real-time PCR assay. Compared with the control groups, the expressions of pre-miR-21 were increased in all the transfected groups. However, upregulation of mature miR-21 was detected only in the wild-type group but not in the Mut1 or Mut2 groups compared with control (Figure 3D). These results suggest that the

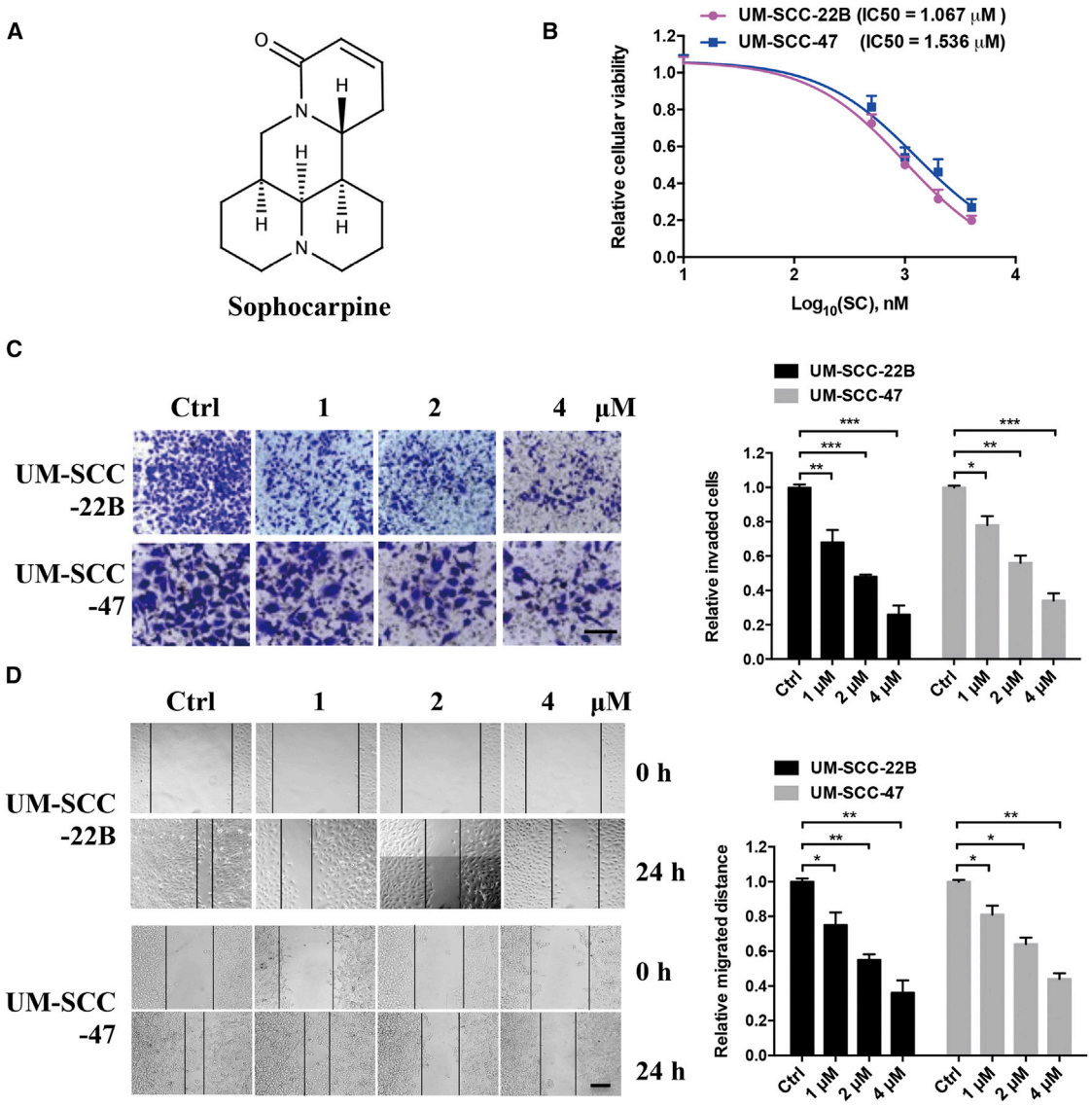

Figure 1. SC Inhibited HNSCC Cell Growth In Vitro

(A) The chemical structure of SC. (B) UM-SCC-22B and UM-SCC-47 cells were treated with increased concentrations of SC for 48 hr. Cell viabilities were evaluated by the CKK-8 assay. (C) Cells were treated with different concentrations of SC for 24 hr and fixed in 95% ethanol and stained with a 4 g/L crystal violet solution. The invaded cells were counted in five randomly selected areas under a 100 × microscope field. Scale bars, 100 μm. (D) The cells were treated as previously, and the wound healing assay was performed to measure the cell migration abilities. Scale bars, 50 μm. Data are shown as mean ± SD of three independent experiments. *$p < 0.05$, **$p < 0.01$, and ***$p < 0.001$ compared with DMSO control.

point mutations of Dicer-binding sites on pre-miR-21 hindered Dicer cleavage of pre-miR-21 to mature miR-21.

To further investigate whether SC inhibit miR-21 expression via specific blockage of Dicer processing, we employed Block-iT Dicer siRNA pools kits against Dicer (si-Dicer, ThermoFisher) to knock-down the expression of Dicer in UM-SCC-22B and UM-SCC-47 cells (Figure 3E). Moreover, the mature miR-21 expression was decreased in si-Dicer transfected cells (Figure 3F). However, combination SC with si-Dicer treatment did not induce a synergetic repression of miR-21 expression, indicating that SC downregulates miR-21 via Dicer functional processing.

P38MAPK Is Involved in SC-Mediated Tumor Cell Progression Inhibition

Given that PTEN is one of the miR-21-validated targets with a vital role in HNSCC,[14,16] we investigated the expression levels of PTEN after SC treatment. As predicted, SC significantly increased PTEN

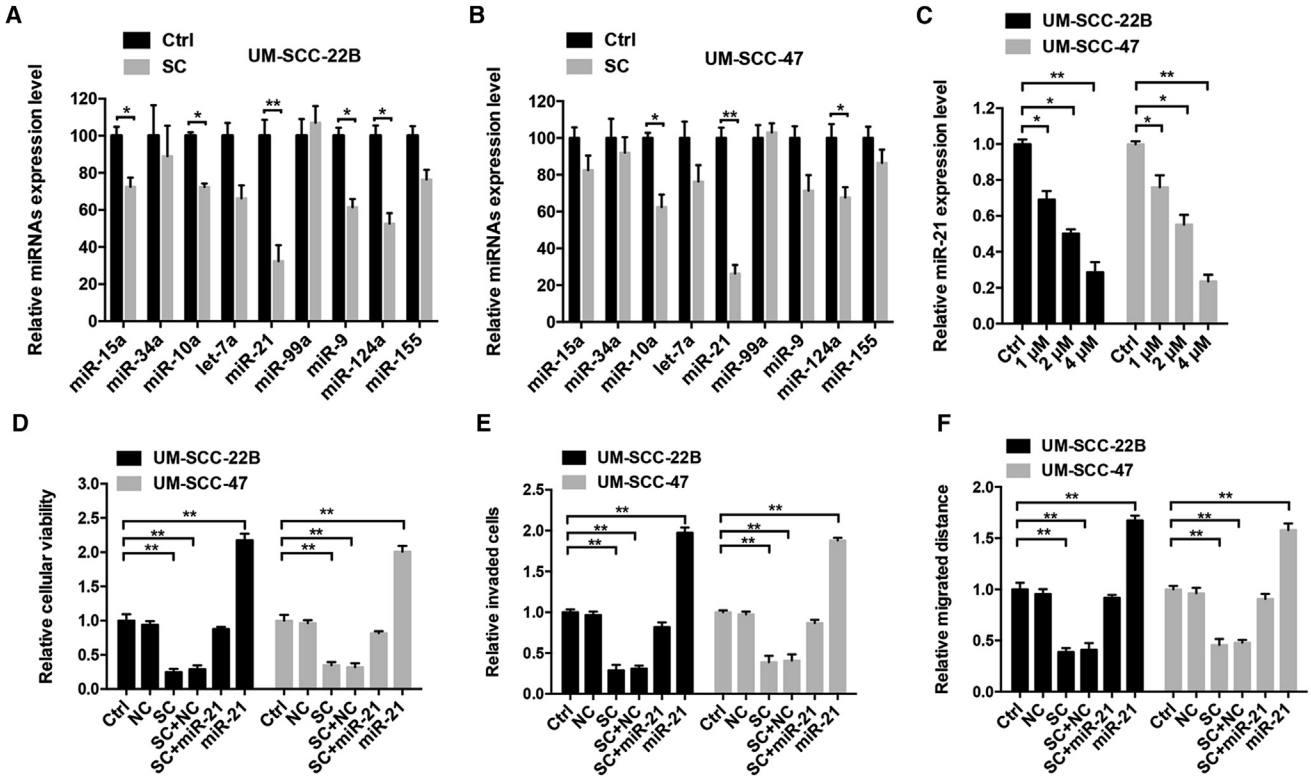

Figure 2. SC Downregulated miR-21 Expression in HNSCC Cells

(A and B) UM-SCC-22B (A) or UM-SCC-47 (B) cells were treated with SC (4 μM) or DMSO for 24 hr. Real-time PCR was then performed to determine the relative expression of the indicated miRNAs. (C) Cells were treated with increased concentrations of SC, and the relative miR-21 expression level was detected using real-time PCR assay. (D–F) The cells were treated with DMSO control (Ctrl), SC (4 μM), RNA negative control (NC), miR-21 mimics (100 nM), or SC with NC or miR-21 mimics (100 nM) for 24 or 48 hr. Then, the relative cell viabilities (D), cell invasion abilities (E), and cell migration abilities (F) were determined using the CKK-8 assay, Transwell assay, and wound healing assays, respectively. Data are shown as mean ± SD of three independent experiments. *$p < 0.05$ and **$p < 0.01$ compared with DMSO control.

protein expression levels in both UM-SCC-22B and UM-SCC-47 cells (Figures 4A and 4B). Moreover, SC upregulated the protein expression of PCDC4, which is also found to be a miR-21 target (Figure S2).[13] We next examined the mechanisms for SC-induced downregulation of miR-21 and inhibition of tumor cell progression. MAPK kinases, including p38, JNK, and ERK, can be activated in response to a wide variety of stimuli in cancers;[17] we therefore asked whether MAPK signal pathways are involved in the mediation of tumor progression induced by SC.

As shown in Figures 4A and 4B, SC treatment activated the phosphorylation of p38MAPK but not ERK or JNK, indicating that the p38MAPK pathway may be involved in the function of SC. To further explore the effect of p38MAPK pathway mediating the process of cell viability, migration, and invasion induced by SC, the p38MAPK specific inhibitor SB203850 was added in cells in combination with SC and then cell viability (Figure 4C), invasion (Figure 4D), and migration (Figure 4E) assays were performed. The inhibition in cells with SC treatment is partially rescued when SB203850 treatment is combined with SC. Furthermore, the decreased expression level of miR-21 induced by SC was also relieved after blocking the p38MAPK signal pathway by SB203850 (Figure 4F). Together, these data indicate that SC can repress the cancer cell viability, invasion, and migration through the p38MAPK signal pathway.

SC Inhibits Epithelial Mesenchymal Transition by Regulating miR-21 Expression

Recent studies have shown that miR-21 can promote EMT in a variety of malignancy tumors, including cholangiocarcinoma and breast cancer.[18–20] Therefore, we try to figure out whether SC exerts its effects on EMT via modulating miR-21 in HNSCC. To this end, the protein and mRNA expression of EMT markers were investigated in UM-SCC-22B and UM-SCC-47 cells. As shown in Figures 5A–5D, SC clearly decreased the expression of mesenchymal marker Vimentin and increased the expression of epithelial marker E-cadherin at both protein and mRNA levels, as determined by western blot (Figures 5A and 5B) and real-time PCR assays (Figures 5C and 5D). In contrary, overexpression of miR-21 by transfection with miR-21 mimics reversed the protein and mRNA expression of Vimentin and E-cadherin markers while combining with SC treatment. Consistent with these results, similar expression changes of Vimentin and E-cadherin were also observed in the immunofluorescence assay following

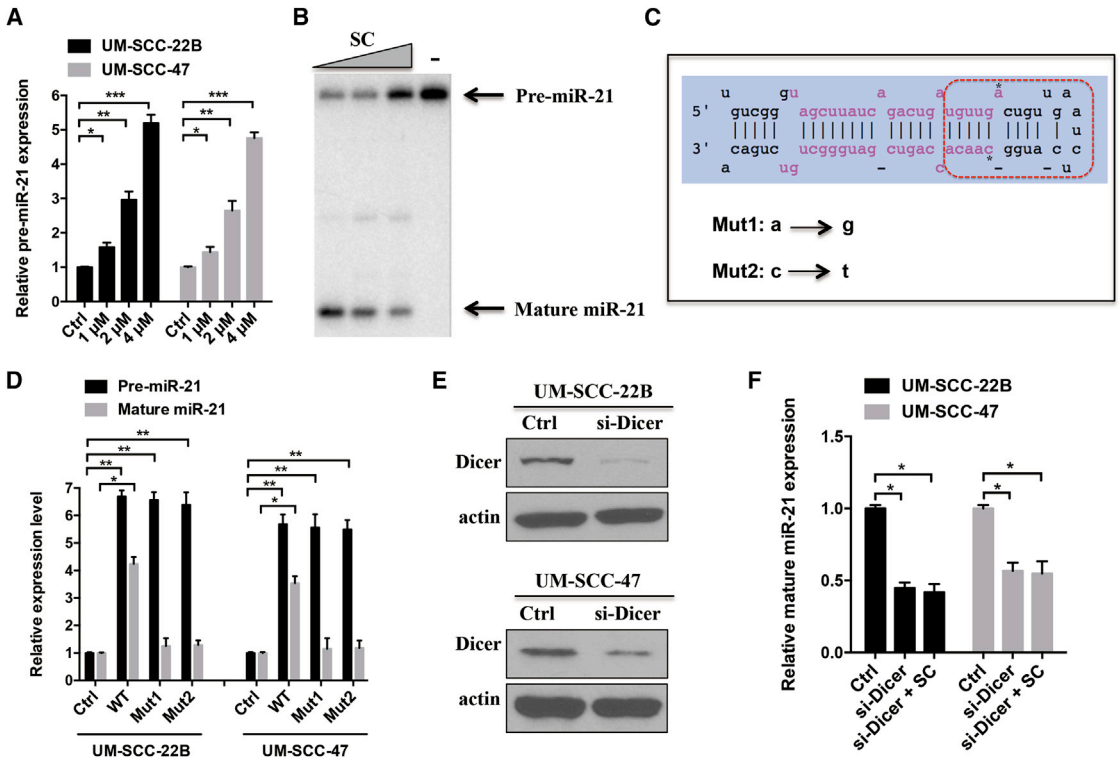

Figure 3. SC Inhibited miR-21 by Blocking Dicer Processing

(A) UM-SCC-22B or UM-SCC-47C cells were treated with increased concentrations of SC and the relative pre-miR-21 expression level was detected using real-time PCR assay. (B) ^{32}P-labeled pre-miR-21 was incubated with recombinant Dicer enzyme in the absence or presence of increased concentrations of SC (1, 2, and 4 μM) for 90 min at 37°C. Then, the samples were run in PAGE gel and exposed to a phosphor screen. (C) The secondary structure of pre-miR-21. The pink bases indicated the mature miR-21 duplex, and the red dotted box indicated the Dicer-binding site on pre-miR-21. Two point mutants of pre-miR-21 RNA oligos were synthesized and shown. The asterisk base (a or c) indicated the mutated base. (D) Real-time PCR was performed to detect the relative expressions of pre-miR-21 and mature miR-21 in cells transfected with wild-type (WT) and two mutant pre-miR-21 RNA (Mut1 and Mut2). (E) Western blot was performed to detect the Dicer expression after transfection with siRNA pools against Dicer (si-Dicer) in cells. Actin was used as the loading control. (F) Real-time PCR detected the mature miR-21 expressions in cells transfected with si-Dicer alone or in combination with SC. Data are shown as mean ± SD of three independent experiments. *$p < 0.05$, **$p < 0.01$, and ***$p < 0.001$ compared with control.

treatment with SC only or with miR-21 (Figures 5E and 5F). In summary, these results suggest that SC inhibits EMT of head and neck cancer cells by modulating miR-21.

SC Inhibits Tumor Growth in UM-SCC-22B Xenografts

The in vivo antitumor effect of SC was further investigated by the development of the UM-SCC-22B xenograft nude mice model. The tumor-bearing mice were intravenously injected with SC (5 mg/kg) or PBS every other day. Tumor volume was measured every 3 days, and tumor weights were determined at autopsy. Throughout the tumorigenic period, the tumor growth in the SC-treated group grew significantly slower than that in the PBS-treated group (Figure 6A; $p < 0.01$). After 21 days, the tumor weights generated from the SC group were significantly decreased compared with those generated from the PBS-treated group (Figure 6B). Moreover, miR-21 expression level from SC-treated tumors was significantly lower than that from control tumors, which is consistent with in vitro results (Figure 6C). No significant body weight loss (Figure 6D) or alanine aminotransferase (ALT) (Figure 6E) and aspartate aminotransferase (AST) (Figure 6F) changes were observed in the treated group during the overall survival time, suggesting no discernible organ toxicities were caused by SC treatment.

In addition, we employed another UM-SCC-22B xenograft mouse model, which was previously developed by our group with cell line engineering with a luciferase reporter containing three repeats of miR-21 target sites at the 3′ UTR of the reporter.[21] The in vivo effect of SC on miR-21 expression was monitored over time in a noninvasive manner using bioluminescence imaging. 48 hr after intravenous administration with SC, the luminescence signal was significantly increased, suggesting SC greatly inhibited miR-21 expression in vivo (Figures 6G and 6H). Furthermore, immunohistochemistry (IHC) staining showed that the expressions of Ki-67 and Vimentin decreased, whereas E-cadherin expression levels were simultaneously increased in the SC-treated group compared with the DMSO-treated control group (Figure 6I). Taken together, our results indicate miR-21 contributed an important role in the anti-tumor effects of SC. The mechanism of SC on the inhibition

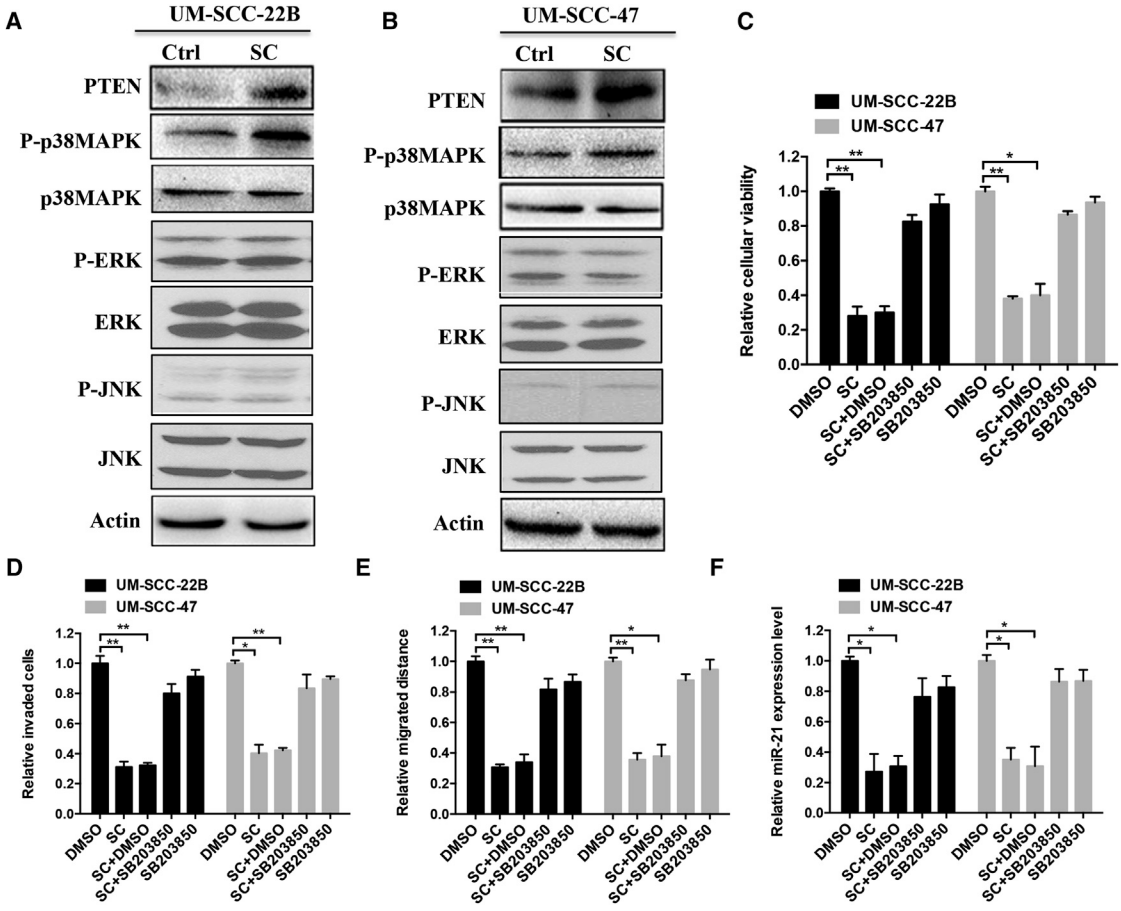

Figure 4. P38MAPK Signaling Is Involved in SC-Mediated Tumor Cell Inhibition

UM-SCC-22B (A) or UM-SCC-47 (B) cells were treated with SC (4 μM) or DMSO for 48 hr. Western blot assay was performed to detect the expressions of the indicated proteins or phosphated proteins. Actin was used as the loading control. (C–F) The cells were treated with DMSO, SC (4 μM), SB203850 inhibitor (10 μM), or SC with DMSO or inhibitor (10 μM) together. Then, the relative cell viabilities (C), cell invasion abilities (D), cell migration abilities (E), and miR-21 expression level (F) were determined using the CKK-8 assay, Transwell assay, wound healing assay, and real-time PCR assay, respectively. Data are shown as mean ± SD of three independent experiments. *$p < 0.05$, **$p < 0.01$, and ***$p < 0.001$ compared with control.

of HNSCC tumor growth by targeting miR-21 is illustrated in Figure 7.

DISCUSSION

In the present study, we demonstrate that SC could efficiently inhibit HNSCC cell proliferation, invasion, and migration in a dose-dependent manner. Moreover, we showed that SC downregulated miR-21 expression by specifically blocking Dicer processing pre-miR-21 to mature miR-21, which is involved in the activation of phosphorylated p38MAPK. By targeting miR-21, SC then upregulates PTEN, one of the miR-21 target genes, and results in the repression of EMT as well as cell growth in HNSCC cells (Figure 7). This implies SC could be a potential miR-21 small-molecule inhibitor and could be used for HNSCC cancer therapy.

Natural products from a variety of natural sources, including microorganisms, animals, and plants, have become the foundation of the treatment of human diseases since ancient times.[22] To date, it is reported that more than 600 natural products exhibit pharmaceutical activity and many of them possess anti-tumor activity.[3] Natural compounds could be used clinically alone or in combination with standard antitumor agents or other natural products. Etoposide, paclitaxel, and vincristine are drugs originating from plant sources. Doxorubicin, mitomycin C, and actinomycin D are classic examples of microbia-derived compounds. Other agents from marine sources, such as Trabectedin (ET-743, Yondelis) and Ara-C (cytarabine, Cytosar-U), have been entered clinical trials for treating liposarcoma or different forms of lymphoma and leukemia.[23] SC is a natural compound originating from the foxtail-like sophoraherb. Recent studies have shown that SC exhibited anti-inflammatory activity on acetic-acid-induced vascular permeability, xylene-induced mouse ear edema, and carrageenan-induced rat paw edema in mice.[6] Another study has found that SC could attenuate non-alcoholic steatohepatitis via inhibition of inflammatory cytokines in rats.[24] Zhang[25] also found

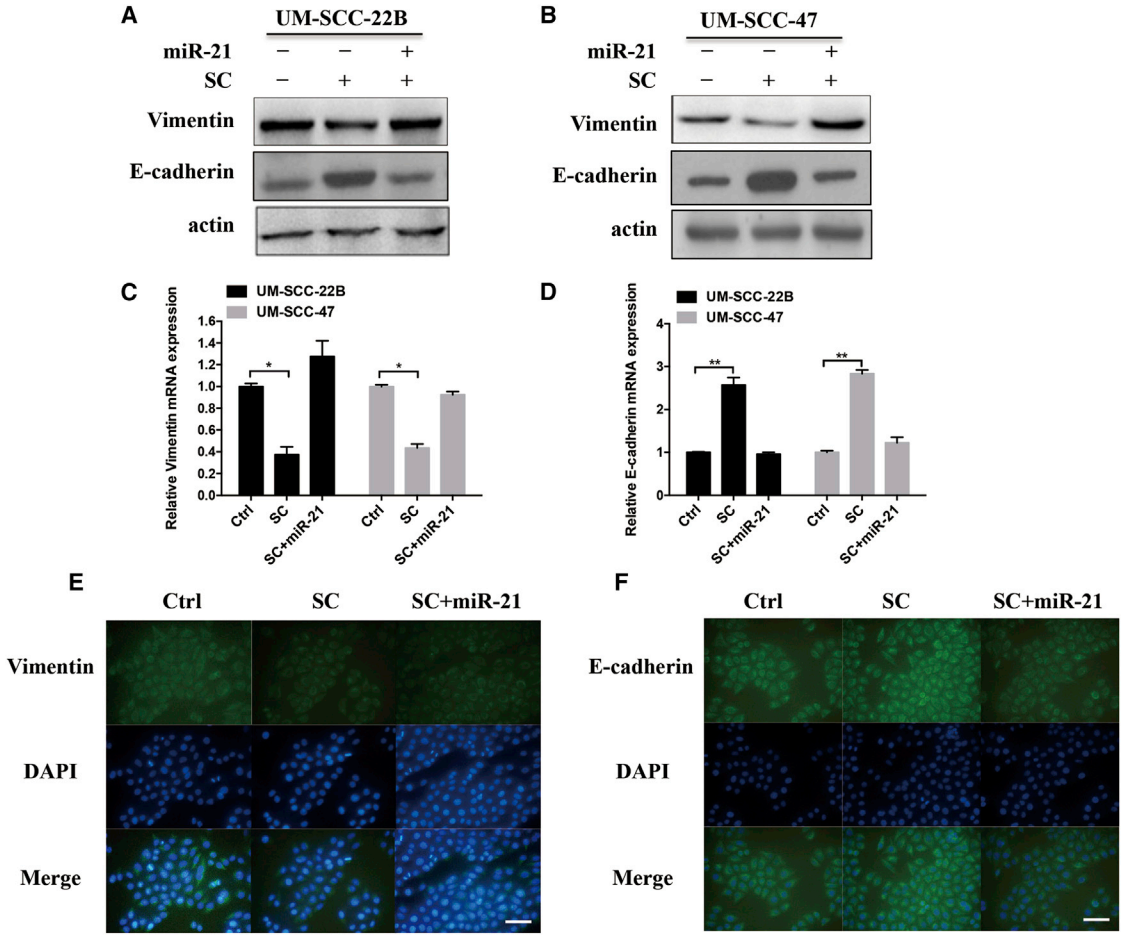

Figure 5. SC Suppressed EMT by Modulating miR-21 Expression

UM-SCC-22B (A) or UM-SCC-47 (B) cells were treated with SC (4 μM) alone or in combination with miR-21 mimics (100 nM) for 48 hr. Western blot assay was performed to determine the protein expression of vimentin or E-cadherin. Actin was used as the loading control. (C and D) Real-time PCR assay was performed to determine the mRNA expression level of vimentin or E-cadherin in both cells. (E and F) Confocal microscopy was used to visualize the vimentin and E-cadherin expression in UM-SCC-22B cells after the same treatment as in (A) and (B). All scale bars, 200 μm. Data are shown as mean ± SD of three independent experiments. *$p < 0.05$ and **$p < 0.01$ compared with control.

that SC exerted its anti-cachectic effects probably via the inhibition of production of tumor necrosis factor alpha (TNF-α) and interleukin-6 (IL-6) in murine macrophages. However, few studies have been carried out to explore the anti-tumor activities and the mechanisms of SC. In this study, we found that SC could efficiently repress HNSCC cell proliferation, invasion, and migration in a dose-dependent manner (Figures 2D–2F). Moreover, SC could remarkably inhibit tumor growth in UM-SCC-22B xenografts (Figures 6A and 6B), providing a promising direction for the anti-tumor effect of SC in HNSCC.

It is of great promise to employ natural products for cancer therapy, not merely because of their toxicity compared with conventional chemotherapeutics, but also because they can target multiple signaling pathways.[26] It is advantageous because tumor transformation and progression is a multi-stage process that is involved in more than one signaling pathway. This can explain why most typical mono-modality therapy fails in cancer therapy because the specific drug usually targets only one single gene in a signaling pathway. The MAPK family, including p38MAPK, ERK, and JNK, has been shown to play a vital role in the mediation of various cellular functions triggered by environmental stress, growth factors, and chemotherapeutics.[27] Increased activity of MAPKs, especially p38MAPK, and their involvement in regulating tumor progression make them promising targets for cancer therapy. Our results demonstrated that the p38MAPK, but not JNK or ERK, signaling pathway is required for the inhibition of tumor cell proliferation, invasion, and migration by SC. Combination treatment with SC and the p38MAPK-specific inhibitor SB203850 rescued the SC-induced repression of cell viability, invasion, and migration (Figures 4C–4E). In contrast, a recent study reported that SC could exert anti-tumor effects in hepatocellular carcinoma, partly by suppressing the activity of the AKT/GSK-3β/β-catenin axis signaling pathways.[28] In addition, Gao et al.[29] showed that SC exhibited anti-inflammatory effects in lipopolysaccharide

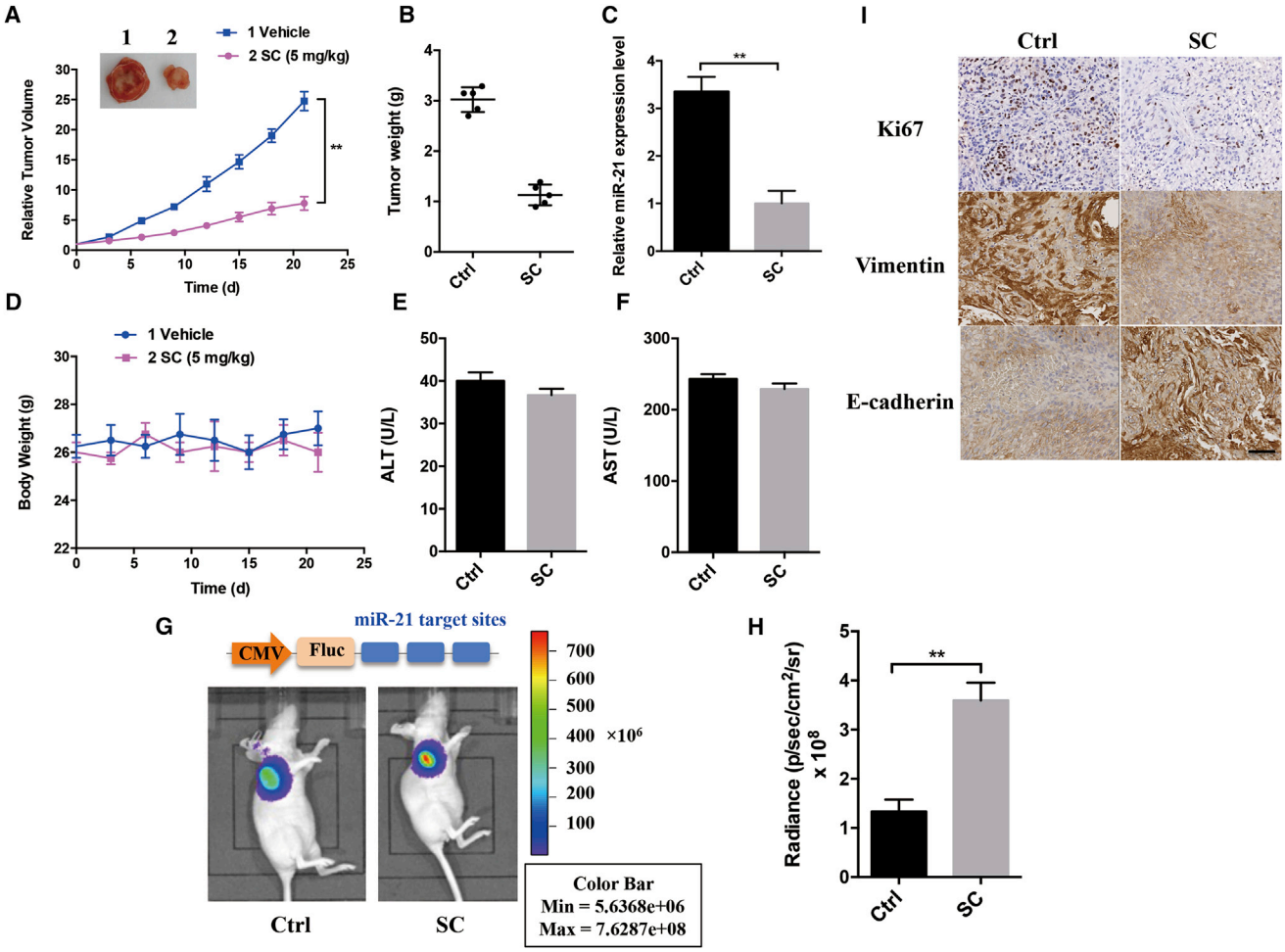

Figure 6. SC Inhibited UM-SCC-22B Xenografted Tumor Growth in Nude Mice

Tumor-bearing xenografted mice were intravenously treated with SC (5 mg/kg) or saline every other day for 3 weeks. Tumor volumes (A), tumor weights (B), and mice body weights (D) were monitored after treatment. (C) MiR-21 expression level was detected in the tumor tissues at autopsy using real-time PCR assay. (E and F) ALT and AST content from mice blood was analyzed. (G and H) After SC treatment for 48 hr, bioluminescence imaging was performed to monitor the luminescence activity from the tumor-bearing xenografted mice developed by luciferase reporter expressing UM-SCC-22B cells. Representative bioluminescence images and the luciferase reporter scheme are shown. (I) Representative photomicrographs of immunohistochemistry are shown to detect Ki-67, vimentin, or E-cadherin expression on tumor sections after SC treatment. Scale bars, 50 μm. Data are shown as mean ± SD of three independent experiments. **$p < 0.01$ compared with control.

(LPS)-induced mouse monocyte macrophage cells via inhibition of p38MAPK and JNK pathways and downregulation of NF-κB activity. Song et al.[8] reported that SC alleviated hepatocyte steatosis by activating the AMPK signaling pathway. Li et al.[7] demonstrated that SC could protect myocardial injury from ischemia reperfusion in rats via NF-κB inactivation and downregulation of JNK and p38. These findings suggest that SC could modulate multiple signaling pathways involving its different biologic functions.

Because natural products exert their anti-tumor effects by targeting numerous signaling pathways and miRNAs could regulate diverse biological processes, such as proliferation, invasion, metastasis, and tumorigenesis, it is believed that miRNAs may function in the regulation response toward natural products. Various studies have documented the specific modulation of miRNA expression profiles following treatment with natural agents, including isoflavone, curcumin, indole-3-carbinol, 3,3′-diindolylmethane, and others, which may result in the increased drug sensitivity of cancer cells and thereby repression of tumor growth.[30] In the present study, we investigated the miRNAs involved in the SC inhibition of tumor cell proliferation, invasion, and metastasis. We found that SC repressed miR-21 expression by specifically blocking Dicer processing of pre-miR-21 to mature miR-21 in a dose-dependent manner (Figures 3A and 3B). Furthermore, overexpression of miR-21 in cells rescued the inhibition of cell proliferation, invasion, and metastasis (Figures 2D–2F) as well as EMT phenotype (Figure 5) induced by SC. On the basis of these observations, we indicated that SC could be a potential miR-21 inhibitor for cancer therapy. Similar with our findings, two small

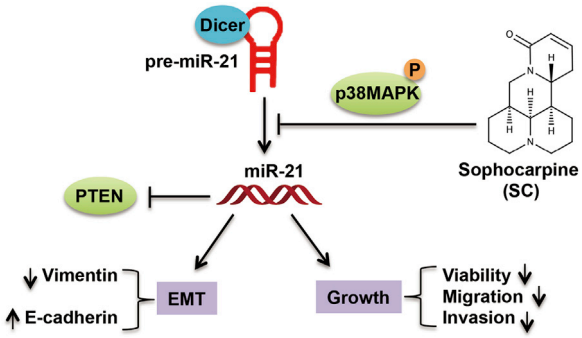

Figure 7. Scheme for Illustrating the Mechanism of SC on HNSCC Cell Growth Inhibition

SC inhibits miR-21 expression via specific blockage of Dicer processing of pre-miR-21 to mature miRNA, which is involved in the phosphorylation of p38MAPK. By targeting miR-21, SC then upregulates PTEN, one of the miR-21 target genes, which results in the inhibition of EMT as well as cell viability, migration, and invasion in HNSCC cells.

molecules, streptomycin[31] and AC1MMYR2,[32] have been shown to interact with pre-miR-21 and inhibit Dicer-mediated processing pre-miR-21 to generate mature miR-21. In contrast, a diazobenzene derivative compound was found to decrease the production of primary miR-21 without affecting downstream mature miR-21 processing by Dicer.[33] Although these small molecule compounds are proven to effectively inhibit miR-21 activity, it is worthy to note that the relative poor in vivo biocompatibility, low water solubility, and high toxicity limit their efficacy as anti-tumor agents for cancer therapies. Therefore, the natural product SC is a much more potent miR-21 inhibitor for prevention and/or treatment of cancers.

In conclusion, we identified a potential miR-21 inhibitor, SC, which shows remarkable repression of HNSCC cell proliferation, invasion, and metastasis, not only through involvement of the p38MAPK signaling pathway, but also through reversibility of the EMT process. Furthermore, SC exhibited robust in vivo antitumor efficacy without any visible toxicity or organ damage to normal tissues, which strengthens its promise as an anticancer agent for HNSCC treatment in the future clinic.

MATERIALS AND METHODS

Reagents and Materials

SC was purchased from Sigma-Aldrich. The signal pathway inhibitors SB203850 were purchased from Beyotime Biotechnology. miR-21 mimics and precursor miR-21 oligos were synthesized from Shanghai GenePharma. The sequences of miR-21 mimics are as follows: 5′-uag cuuaucagacugauguuga-3′ (forward strand); 5′-caacaccagucgaugggc ugu-3′ (reverse strand). The sequences of precursor miR-21 are as follows: 5′-ugucggguagcuuaucagacugauguugacuguugaaucucauggcaa cac cagucgaugggcugucugaca-3′. The siRNA pools for Dicer knockdown were generated from Block-iT Dicer kits (Thermo Fisher Scientific), which provide highly effective siRNAs pools for Dicer knockdown.

Cell Lines and Transfection

The UM-SCC-22B and UM-SCC-47 cells were purchased from Cell Bank of Chinese Academy of Sciences. Cells were cultured in DMEM and supplemented with 10% fetal bovine serum (FBS) and 1% glutamine. miRNA mimics or siRNAs were transfected with Lipofectamine RNAiMAX (Invitrogen) according to the manufacturer's protocols.

Real-Time PCR

Total RNA was extracted from tissues or cultured cells with TRIzol (Invitrogen) for miRNA or mRNA analysis. To determine the level of mature miRNA, we used a stem-loop RT primer. Total RNA was polyadenylated using a stem-loop-based First Strand Synthesis kit (BioTeke Corporation) according to the manufacturer's product manual. Then, real-time RT-PCR was performed with a SYBR Premix Ex Taq miRNA kit (TaKaRa) in accordance with the manufacturer's instructions. U6 small nuclear RNA was used as an internal control for miRNA detection. Actin was used as control for detecting other genes. All measurements were performed three times. All primer sequences are listed in Table S1.

Western Blot

The cells were harvested and lysed in RIPA lysis buffer (Beyotime Biotechnology) at room temperature for 10 min. The supernatants were collected, and the protein concentrations were determined using a BCA protein assay kit (Beyotime Biotechnology). Then, equal amounts of protein extracts (20 μg) were loaded in the SDS-PAGE gel and then transferred to polyvinylidene difluoride (PVDF) membranes. After blocking with 5% BSA for 1 hr at room temperature, the transferred membranes were incubated with primary antibodies for 1 hr at room temperature, and then incubated with the secondary antibodies for another 1 hr. Finally, the immunoreactivity was detected using the ECL detecting instrument (GE Healthcare Bio-Sciences). The primary and secondary antibodies were purchased from Santa Cruz Biotechnology. The protein bands were quantified using ImageJ software and normalized to the signal intensity of actin.

Cell Viability Assay

The cell viability effect of SC was determined using a cell counting kit-8 (CKK8, Beyotime Biotechnology) according to the manufacturer's protocols. Briefly, cells were seeded in a 96-well plate (5×10^3 cells/well) and treated with different reagents for another 48 hr. Then, 10 μL of CKK-8 was added to each well for 4 hr and the absorbance at 450 nm was measured with a microplate reader (Synergy HT, Biotech). The OD values were determined to reflect the viable cell population from each well.

Wound Scratch Assay

Cells were treated with different reagents as indicated; then, cell layers were scratched using a 20-μL sterile pipette tip to form wound gaps. Cells were captured to record the wound width as 0 hr time point. Cells were cultured in serum-free medium and then photographed after 24 hr to record the cell migration wound.

Transwell Assay

Cell invasion was detected using Transwell chambers (8-μm pore size; Millipore). In brief, 600 μL of complete medium was added to the bottom chamber, transfected cells were suspended in serum-free medium, and 200 μL of cell suspension (containing 4×10^4 cells) was placed in the upper chamber. After 24 hr, the cells on the top surface of the membrane were mechanically removed using a cotton swab, and the cells on the bottom surface of the membrane were fixed in 95% ethanol and stained with 4 g/L crystal violet solution. Cells adhering to the bottom surface of the membrane were counted in five randomly selected areas under a 100 × microscope field. Each experiment was repeated three times. All data were normalized with a control chamber that contains cells with no treatment.

Immunofluorescence and Immunohistochemistry Assay

Immunofluorescence staining was performed using antibodies against E-cadherin and Vimentin (1:500 dilutions; Cell Signaling Technology), and the cells were visualized under Leica confocal microscopes. For the immunohistochemistry assay, tissue sections were incubated with specific antibodies against Ki-67, E-cadherin, and Vimentin (1:500 dilutions; Cell Signaling Technology) overnight at 4°C. Cells were visualized using a light microscope.

Dicer Blocking Assay

^{32}P-5′ end-labeled RNA (~50 ng) was incubated in 10 mM NaCl (pH 7.5), 1 mM $MgCl_2$, and 10 mM sodium cacodylate buffer in a total volume of 10 μL. Then, the mixture was heated at 95°C for 5 min for denaturing, followed by cooling to 37°C. A different concentration of SC was then added and incubated for 30 min, followed by addition of 0.5 U of recombinant Dicer enzyme (Amsbio). The reaction was performed at 37°C for 90 min, and stopped by the Dicer stop buffer (Amsbio). Then, the sample was run in a 15% denaturing PAGE after the addition of loading dye. Finally, the gel was exposed to a phosphor screen and the image was visualized using the Typhoon trio phosphoimager.

Mice Blood Analysis

Whole blood (200 μL) from mice was harvested in EDTA-coated tubes via cardiac puncture of anesthetized mice. Samples were analyzed for ALT and AST using an ALT activity assay kit or AST activity assay kit (Sigma) according to the manufacturer's protocols.

Animal Studies

All animal experiments were performed with the Guild for the Care and Use of Laboratory Animals according to animal protocols approved by Xidian University and Forth Military Medical University. Xenografted tumor models were prepared by injection of 1×10^7 UM-SCC-22B cells suspended in PBS into a nude mouse (n = 5). After tumors reached a volume of about 100 mm^3, SC (5 mg/kg) was intravenously injected into mice. For the anti-tumor therapy studies, tumor-bearing mice (n = 5) intravenously received 5 mg/kg of SC every other day, whereas the control group of mice (n = 6) received saline only. After injection for 21 days, mice were sacrificed to harvest tumors. Tumor growth measurement was calculated as $LW^2/2$, where L indicates the long diameter and W indicates the short diameter.

For in vivo bioluminescence imaging, xenografted tumor models were developed by injection of 1×10^7 UM-SCC-22B cells expressing luciferase reporter genes into the nude mice (n = 5). After tumors had grown up to about 200 mm^3, the animals were given SC intravenously (5 mg/kg). At 0 and 48 hr after treatment, the animals were injected with substrate D-luciferin (150 mg/kg) and were then anesthetized with 2% isoflurane for bioluminescence imaging. The images were taken using a Xenogen Lumina Π system for 5 min. The luminescence intensity was expressed as $p/s/cm^2/sr$ using Living Image software 4.1 (Xenogen).

Statistical Analysis

All data are presented as mean ± SD. The differences between means were analyzed with a t test. All statistical analyses were performed using SPSS version 17.0 (IBM), and all figures were generated using GraphPad Prism 5.01 (GraphPad Software). $p < 0.05$ was considered statistically significant.

SUPPLEMENTAL INFORMATION

Supplemental Information includes two figures and one table and can be found with this article online at http://dx.doi.org/10.1016/j.ymthe.2017.05.008.

AUTHOR CONTRIBUTIONS

Conceptualization, F.W.; Methodology, F.W.; Investigation, W.L., B.Z., G.C., W.W., L.Z., Y.S., Y.L., and Y.S.; Resources, Q.Z.; Writing – Original Draft, F.W.; Writing – Review and Editing, F.W. and X.D.; Funding Acquisition, F.W.; Project Administration, F.W.

CONFLICTS OF INTEREST

The authors declare no conflict of interest.

ACKNOWLEDGMENTS

This work was supported by the National Natural Science Foundation of China (grant No. 81571721, 81227901, 81301214, and 31400662), National Basic Research and Development Program of China (973 Program) (grant No. 2013CB733803), and Natural Science Basis Research Plan in Shaanxi Province of China (program No. 2016JM8016 and 2013JQ4040).

REFERENCES

1. Siegel, R.L., Miller, K.D., and Jemal, A. (2016). Cancer statistics, 2016. CA Cancer J. Clin. *66*, 7–30.

2. Khuri, F.R., Kim, E.S., Lee, J.J., Winn, R.J., Benner, S.E., Lippman, S.M., Fu, K.K., Cooper, J.S., Vokes, E.E., Chamberlain, R.M., et al. (2001). The impact of smoking status, disease stage, and index tumor site on second primary tumor incidence and tumor recurrence in the head and neck retinoid chemoprevention trial. Cancer Epidemiol. Biomarkers Prev. *10*, 823–829.

3. Nobili, S., Lippi, D., Witort, E., Donnini, M., Bausi, L., Mini, E., and Capaccioli, S. (2009). Natural compounds for cancer treatment and prevention. Pharmacol. Res. *59*, 365–378.

4. Butler, M.S. (2008). Natural products to drugs: natural product-derived compounds in clinical trials. Nat. Prod. Rep. *25*, 475–516.
5. Agbarya, A., Ruimi, N., Epelbaum, R., Ben-Arye, E., and Mahajna, J. (2014). Natural products as potential cancer therapy enhancers: A preclinical update. SAGE Open Med. *2*, 2050312114546924.
6. Gao, Y., Li, G., Li, C., Zhu, X., Li, M., Fu, C., and Li, B. (2009). Anti-nociceptive and anti-inflammatory activity of sophocarpine. J. Ethnopharmacol. *125*, 324–329.
7. Li, C., Gao, Y., Tian, J., Shen, J., Xing, Y., and Liu, Z. (2011). Sophocarpine administration preserves myocardial function from ischemia-reperfusion in rats via NF-κB inactivation. J. Ethnopharmacol. *135*, 620–625.
8. Song, C.Y., Shi, J., Zeng, X., Zhang, Y., Xie, W.F., and Chen, Y.X. (2013). Sophocarpine alleviates hepatocyte steatosis through activating AMPK signaling pathway. Toxicol. In Vitro *27*, 1065–1071.
9. Ha, M., and Kim, V.N. (2014). Regulation of microRNA biogenesis. Nat. Rev. Mol. Cell Biol. *15*, 509–524.
10. Ameres, S.L., and Zamore, P.D. (2013). Diversifying microRNA sequence and function. Nat. Rev. Mol. Cell Biol. *14*, 475–488.
11. Lu, J., Getz, G., Miska, E.A., Alvarez-Saavedra, E., Lamb, J., Peck, D., Sweet-Cordero, A., Ebert, B.L., Mak, R.H., Ferrando, A.A., et al. (2005). MicroRNA expression profiles classify human cancers. Nature *435*, 834–838.
12. Krichevsky, A.M., and Gabriely, G. (2009). miR-21: a small multi-faceted RNA. J. Cell. Mol. Med. *13*, 39–53.
13. Asangani, I.A., Rasheed, S.A., Nikolova, D.A., Leupold, J.H., Colburn, N.H., Post, S., and Allgayer, H. (2008). MicroRNA-21 (miR-21) post-transcriptionally downregulates tumor suppressor Pdcd4 and stimulates invasion, intravasation and metastasis in colorectal cancer. Oncogene *27*, 2128–2136.
14. Meng, F., Henson, R., Wehbe-Janek, H., Ghoshal, K., Jacob, S.T., and Patel, T. (2007). MicroRNA-21 regulates expression of the PTEN tumor suppressor gene in human hepatocellular cancer. Gastroenterology *133*, 647–658.
15. Shenouda, S.K., and Alahari, S.K. (2009). MicroRNA function in cancer: oncogene or a tumor suppressor? Cancer Metastasis Rev. *28*, 369–378.
16. Squarize, C.H., Castilho, R.M., Abrahao, A.C., Molinolo, A., Lingen, M.W., and Gutkind, J.S. (2013). PTEN deficiency contributes to the development and progression of head and neck cancer. Neoplasia *15*, 461–471.
17. Dhillon, A.S., Hagan, S., Rath, O., and Kolch, W. (2007). MAP kinase signalling pathways in cancer. Oncogene *26*, 3279–3290.
18. De Mattos-Arruda, L., Bottai, G., Nuciforo, P.G., Di Tommaso, L., Giovannetti, E., Peg, V., Losurdo, A., Pérez-Garcia, J., Masci, G., Corsi, F., et al. (2015). MicroRNA-21 links epithelial-to-mesenchymal transition and inflammatory signals to confer resistance to neoadjuvant trastuzumab and chemotherapy in HER2-positive breast cancer patients. Oncotarget *6*, 37269–37280.
19. Han, M., Wang, Y., Liu, M., Bi, X., Bao, J., Zeng, N., Zhu, Z., Mo, Z., Wu, C., and Chen, X. (2012). MiR-21 regulates epithelial-mesenchymal transition phenotype and hypoxia-inducible factor-1α expression in third-sphere forming breast cancer stem cell-like cells. Cancer Sci. *103*, 1058–1064.
20. Liu, Z., Jin, Z.Y., Liu, C.H., Xie, F., Lin, X.S., and Huang, Q. (2015). MicroRNA-21 regulates biological behavior by inducing EMT in human cholangiocarcinoma. Int. J. Clin. Exp. Pathol. *8*, 4684–4694.
21. Wang, F., Zhang, B., Zhou, L., Shi, Y., Li, Z., Xia, Y., and Tian, J. (2016). Imaging dendrimer-grafted graphene oxide mediated anti-miR-21 delivery with an activatable luciferase reporter. ACS Appl. Mater. Interfaces *8*, 9014–9021.
22. Khazir, J., Riley, D.L., Pilcher, L.A., De-Maayer, P., and Mir, B.A. (2014). Anticancer agents from diverse natural sources. Nat. Prod. Commun. *9*, 1655–1669.
23. Catalani, E., Proietti Serafini, F., Zecchini, S., Picchietti, S., Fausto, A.M., Marcantoni, E., Buonanno, F., Ortenzi, C., Perrotta, C., and Cervia, D. (2016). Natural products from aquatic eukaryotic microorganisms for cancer therapy: perspectives on anti-tumour properties of ciliate bioactive molecules. Pharmacol. Res. *113* (Pt A), 409–420.
24. Song, C.Y., Zeng, X., Chen, S.W., Hu, P.F., Zheng, Z.W., Ning, B.F., Shi, J., Xie, W.F., and Chen, Y.X. (2011). Sophocarpine alleviates non-alcoholic steatohepatitis in rats. J. Gastroenterol. Hepatol. *26*, 765–774.
25. Zhang, Y., Wang, S., Li, Y., Xiao, Z., Hu, Z., and Zhang, J. (2008). Sophocarpine and matrine inhibit the production of TNF-alpha and IL-6 in murine macrophages and prevent cachexia-related symptoms induced by colon26 adenocarcinoma in mice. Int. Immunopharmacol. *8*, 1767–1772.
26. Butler, M.S., Robertson, A.A., and Cooper, M.A. (2014). Natural product and natural product derived drugs in clinical trials. Nat. Prod. Rep. *31*, 1612–1661.
27. Reibman, J., Talbot, A.T., Hsu, Y., Ou, G., Jover, J., Nilsen, D., and Pillinger, M.H. (2000). Regulation of expression of granulocyte-macrophage colony-stimulating factor in human bronchial epithelial cells: roles of protein kinase C and mitogen-activated protein kinases. J. Immunol. *165*, 1618–1625.
28. Zhang, P.P., Wang, P.Q., Qiao, C.P., Zhang, Q., Zhang, J.P., Chen, F., Zhang, X., Xie, W.F., Yuan, Z.L., Li, Z.S., et al. (2016). Differentiation therapy of hepatocellular carcinoma by inhibiting the activity of AKT/GSK-3β/β-catenin axis and TGF-β induced EMT with sophocarpine. Cancer Lett. *376*, 95–103.
29. Gao, Y., Jiang, W., Dong, C., Li, C., Fu, X., Min, L., Tian, J., Jin, H., and Shen, J. (2012). Anti-inflammatory effects of sophocarpine in LPS-induced RAW 264.7 cells via NF-κB and MAPKs signaling pathways. Toxicol. In Vitro *26*, 1–6.
30. Li, Y., Kong, D., Wang, Z., and Sarkar, F.H. (2010). Regulation of microRNAs by natural agents: an emerging field in chemoprevention and chemotherapy research. Pharm. Res. *27*, 1027–1041.
31. Bose, D., Jayaraj, G., Suryawanshi, H., Agarwala, P., Pore, S.K., Banerjee, R., and Maiti, S. (2012). The tuberculosis drug streptomycin as a potential cancer therapeutic: inhibition of miR-21 function by directly targeting its precursor. Angew. Chem. Int. Ed. Engl. *51*, 1019–1023.
32. Shi, Z., Zhang, J., Qian, X., Han, L., Zhang, K., Chen, L., Liu, J., Ren, Y., Yang, M., Zhang, A., et al. (2013). AC1MMYR2, an inhibitor of dicer-mediated biogenesis of Oncomir miR-21, reverses epithelial-mesenchymal transition and suppresses tumor growth and progression. Cancer Res. *73*, 5519–5531.
33. Gumireddy, K., Young, D.D., Xiong, X., Hogenesch, J.B., Huang, Q., and Deiters, A. (2008). Small-molecule inhibitors of microrna miR-21 function. Angew. Chem. Int. Ed. Engl. *47*, 7482–7484.

YMTHE, Volume *25*

Supplemental Information

Targeting miR-21 with Sophocarpine Inhibits Tumor Progression and Reverses Epithelial-Mesenchymal Transition in Head and Neck Cancer

Wei Liu, Beilei Zhang, Guo Chen, Wenjiao Wu, Lin Zhou, Yaru Shi, Qi Zeng, Yanqiu Li, Youwei Sun, Xingming Deng, and Fu Wang

Supplemental Information

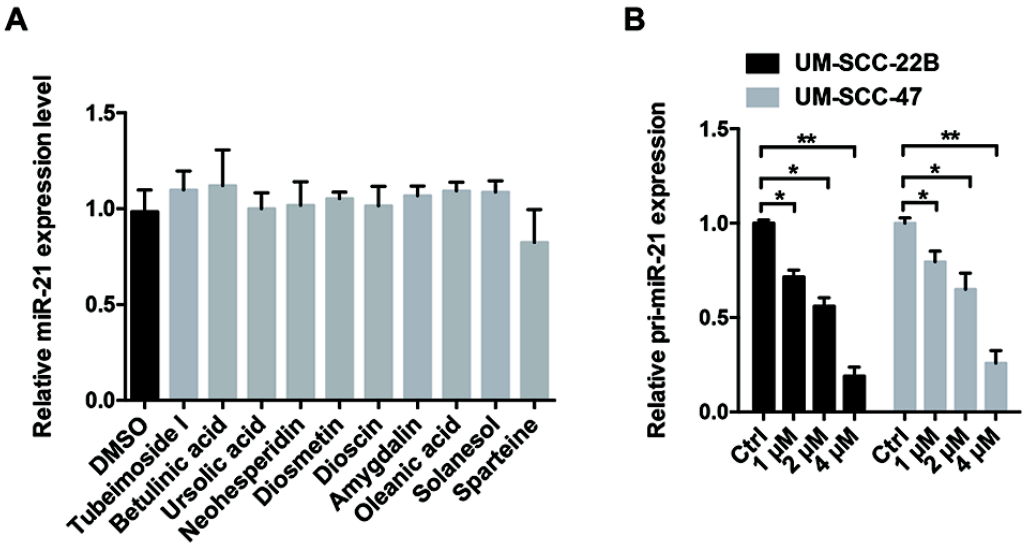

Figure S1. (A) UM-SCC-22B was treated with 10 different natural agents (4 μM) as indicated for 48 h. Then real-time PCR was performed to detect the expression of miR-21. (B) UM-SCC-22B or UM-SCC-47 cells were treated with increased concentrations of SC and the relative miR-21 expression level was detected using real-time PCR assay. Data are shown as mean ± SD of three independent experiments. *P < 0.05, **P < 0.01 compared with DMSO control.

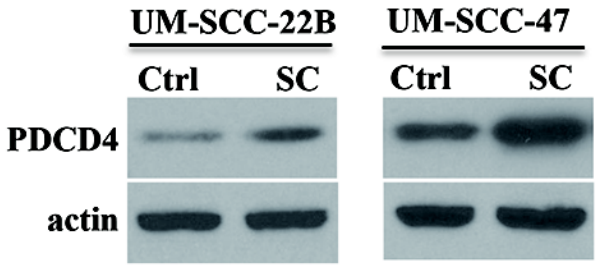

Figure S2. UM-SCC-22B or UM-SCC-47 cells were treated with SC (4 μM) or DMSO for 48 h. Western blot assay was performed to detect the protein expressions of PDCD4. Actin as used as the loading control.

Table S1. Primer sequences for qPCR

Primer name	**Primer sequence (5'-3')**
Vimentin-F	GACGCCATCAACACCGAGTT
Vimentin-R	CTTTGTCGTTGGTTAGCTGGT
E-cadherin-F	CGGTGGTCAAAGAGCCCTTACT
E-cadherin-R	TGAGGGTTGGTGCAACAACGTCGTTA
Actin-F	AACAAGAGGCCACACAAATAGG
Actin-R	CAGATGTACAGGAATAGCCTCCG
U6-F	CAGGGGCCATGCTAAATCTTC
U6-R	CTTCGGCAGCACATATACTAAAAT
mir21-F	GTAGCTTATCAGACTGATGTTGA
mir10a-F	TACCCTGTAGATCCGAATTTGTG
mir15a-F	TAGCAGCACATAATGGTTTGTG
mir99a-F	AACCCGTAGATCCGATCTTGTG
mir124a-F	TAAGGCACGCGGTGAATGCC
mir155-F	TTAATGCTAATCGTGATAGGGGT
mir34a-F	TGGCAGTGTCTTAGCTGGTTGT
mir9-F	TCTTTGGTTATCTAGCTGTATGA
let7a-F	TGAGGTAGTAGGTTGTATAGTT